ARTICLES

Geometry Optimization of Carbon Dioxide Clusters $(CO_2)_n$ for $4 \leq n \leq 40$

Hiroshi Takeuchi†

Division of Chemistry, Graduate School of Science, Hokkaido University, Sapporo 060-0810

Received: April 3, 2008; Revised Manuscript Received: June 13, 2008

Geometry optimization of carbon dioxide clusters $(CO_2)_n$ with the size of $4 \leq n \leq 40$ is performed by a heuristic and unbiased method combined with geometrical perturbations. Comparison with the global minima reported in the literature shows that the present method reproduces the global minima for clusters with $n =$ 6, 8, 13, 19, 28, 30, and 32 and yields new global minima for $(CO_2)_{23}$, $(CO_2)_{25}$, and $(CO_2)_{35}$. For the other clusters under investigation, global minima are first reported in this article. Structural features of CO_2 clusters and efficiency of the optimization method are discussed.

Introduction

It is difficult to estimate optimal geometries of clusters of finite atoms or molecules theoretically because of the enormous number of stable geometries. Therefore, determination of global-minimum structures of clusters is a challenging problem in theoretical chemistry. Recently, the present author proposed a heuristic and unbiased method for geometry optimization of Lennard-Jones (LJ) atomic clusters.[1] The proposed method yielded putative global minima for LJ_{10} to LJ_{561} reported in the literature[2–9] with reducing computational effort compared with previous unbiased methods. Moreover, it was possible to find new global minima for LJ_{506}, LJ_{521}, LJ_{536}, LJ_{537}, LJ_{538} and LJ_{541}. The method was modified to treat a more complicated problem, geometry optimization of clusters consisting of nonspherical molecules. To illustrate performance of the method, geometries of benzene clusters $(C_6H_6)_n$ up to 30 molecules were optimized.[10] Comparison of the obtained results with the data in the literature[11–16] showed that global minima for clusters of 11, 14, and 15 molecules were improved and that global minima for $16 \leq n \leq 30$ were first evaluated. Therefore, the method takes high efficiency for geometry optimization of molecular clusters as well as atomic clusters. The purpose of the present study is to apply the above method to carbon dioxide clusters $(CO_2)_n$.

Bukowski et al.[17] performed ab initio calculations to obtain an intermolecular potential of the CO_2 dimer. In the investigation, geometries of the dimer and trimer were predicted with ab initio and empirical potentials. Geometries of $(CO_2)_n$ clusters for $n \geq 4$ were investigated[18–21] with the empirical intermolecular potential of Murthy, O'Shea, and McDonald (MOM).[22] Liu and Jordan[18] used the parallel-tempering Monte Carlo procedure to characterize the $(CO_2)_n$, $n =$ 6, 8, 13, and 19, clusters. Maillet et al.[19,20] carried out molecular dynamics (MD) calculations to investigate the structures of $(CO_2)_n$ with $n =$ 13, 19, 23, 28, 30, 32, 35, and 55. Torchet et al.[21] studied structures of CO_2 clusters by means of electron diffraction with the aid of MD simulations. In the study by van de Waal,[23] a different empirical potential was used to estimate structures of $(CO_2)_n$ from 13-, 19-, 55-, 147-, 309-, and 561-molecule fragments of the crystal structure. The present study reports a set of putative global minima of $(CO_2)_n$ with $n \leq 40$ described by the MOM potential to examine size dependence of the cluster geometries. In the MOM model, molecular structure of carbon dioxide is rigid (r(C═O) = 1.16 Å and ∠OCO = 180°), five partial charges are located on the molecular axis, and the intermolecular potential consists of electrostatic and LJ atom-atom terms. The LJ parameters and partial charges are summarized in refs 18 and 19.

Method

Searches for optimal geometries are based on the heuristic algorithm combined with geometrical perturbations.[10] In the first stage of the algorithm, molecules are randomly placed in a sphere having a radius of $R = (3n/4\pi)^{1/3} r_e$, where r_e denotes the distance between equilibrium positions of two molecules (4.99 Å).[24] The initial geometry is locally optimized by using a quasi-Newton method (the L-BFGS[25] method is used throughout). The optimized geometry is then modified by using interior (*I*), surface (*S*), and orientational (*O*) operators in that order. The *I* operator gives a perturbation on a cluster configuration by moving some outer molecules to the neighborhood of the center of mass of a cluster, the *S* operator modifies a cluster configuration by moving them to the most stable positions on the surface of a cluster, and the *O* operator randomizes orientational degrees of freedom of all the molecules in a cluster. Geometries modified according to these operators are optimized with the L-BFGS[25] method. The algorithm used in the present method is summarized in Figure 1. The details of the algorithm are described below.

Selection of Outer Molecules. The highest-energy group consisting of *m* outer molecules is generally selected and then moved by the *I* and *S* operators where *m* is a predetermined value as described below. The selection is performed as follows.[10] For all the combinations of *m* molecules on the outer shell of the cluster (numbering of molecules is represented by

† Phone: +81-11-706-3533. Fax: +81-11-706-3501. E-mail: takehi@sci.hokudai.ac.jp.

10.1021/jp802872p CCC: $40.75
Published on Web 07/30/2008

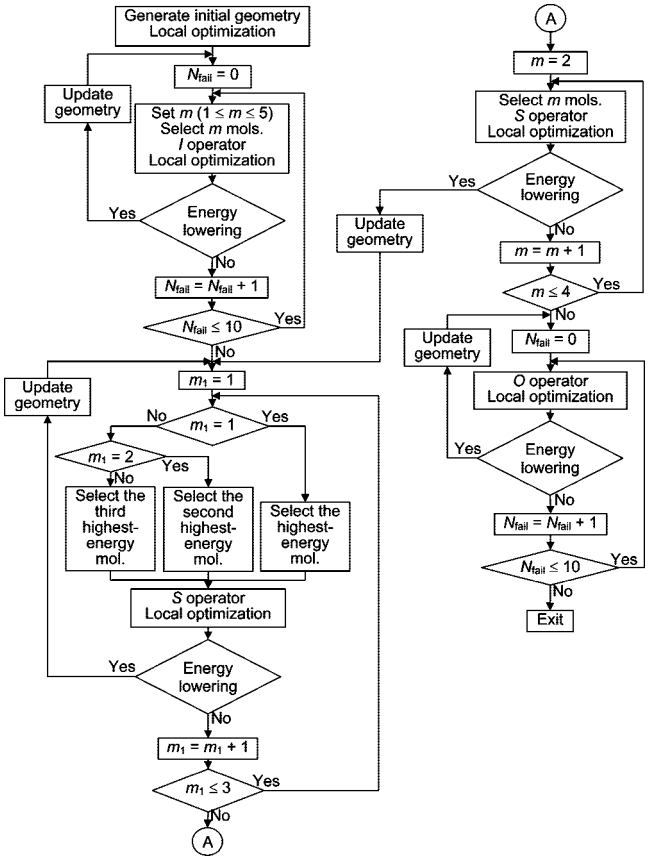

Figure 1. Optimization cycle proposed for molecular clusters.

$k_1, k_2, ..., k_m$), the contribution $E_{select}(k_1, k_2, ..., k_m)$ of these molecules to the energy of the cluster is calculated by the formula

$$E_{select}(k_1, k_2, ..., k_m) = \sum_{i=1}^{m} \sum_{j \neq k_i}^{n} E(k_i, j) - \sum_{i=1}^{m-1} \sum_{j=i+1}^{m} E(k_i, k_j) \quad (1)$$

Here $E(i,j)$ denotes the MOM potential energy between ith and jth molecules. By referring to all the E_{select} values, the combination with the highest energy is selected.

Interior Operator. The number of m is randomly selected from 1 to 5.[10] The selected molecules are moved on the surface of the sphere whose center coincides with the center of mass of the cluster. The radius of the sphere is fixed at $r_e/2$. Orientations of the moved molecules are randomly determined. Recently, Shao et al.[26] used a similar operator in geometry optimization of large LJ clusters and analyzed performance of the I operator by examining the structural variation due to this operator.

The previous studies on LJ and benzene clusters[1,10] indicated that energies of clusters were significantly improved by using the I operator. Therefore, this operator is carried out prior to the S and O operators.

If the energy of a cluster is not improved by using this operator during the last 10 local optimizations, calculation proceeds to next step (see Figure 1). Otherwise, the cluster geometry is updated and the operator is repeatedly performed. The O operator also takes this procedure.

Surface Operator. The highest-energy molecule or group is moved on the surface of the cluster. The number m is initially set at 1. It increases to 4 at an interval of 1 when the energy of a cluster is not lowered by using this operator.[10] If the energy is improved, the cluster geometry is updated and m is again set at 1.

The most stable set of positions on the surface is selected as the positions of the moved molecules. The following procedure is used to search it:[10] (1) Remove the m molecules from the cluster and prepare the template cluster composed of the $(n-m)$ molecules. (2) Add a molecule on the surface of the template cluster at random, optimize position and orientation of the added molecule, and sort its position and orientation (S) and the potential energy between the molecule and the template $E_{template}(S)$. This is repeated $3n$ times to create a list of distinct spaces.[27] (3) Calculate the energy $E_{surface}$ for all the combinations of m spaces in the list by

$$E_{surface}(S_1, S_2, ..., S_m) = \sum_{i=1}^{m} E_{template}(S_i) + \sum_{i=1}^{m-1} \sum_{j=i+1}^{m} E(S_i, S_j) \quad (2)$$

where m spaces are represented by $S_1, S_2, ..., S_m$ and $E_{template}(S_i)$ is obtained in step 2. The combination must be different from that of the spaces of the molecules removed in step 1. (4) From all the combinations, search the combination with the lowest potential energy $E_{surface}^{min}$. (5) When $m \ge 2$,[28] for all the configurations with energies less than $E_{surface}^{min} + 5.0$ kJ mol^{-1}, the positions and orientations of m molecules are simultaneously optimized. (6) The positions and orientations giving the lowest energy are used for those of the moved molecules.

In the S operator with $m = 1$, the second highest-energy molecule and the third highest-energy molecule are also selected as a moved molecule (see the steps with $m_1 = 2, 3$ in Figure 1). This was efficient for searching optimal geometries of CO_2 clusters as well as LJ and benzene clusters.[1,10]

Orientational Operator. This randomizes orientations of all molecules in a cluster but the centers of mass of the molecules are fixed. Geometrical modification due to this operator does not occur in geometrical perturbations caused by the I and S operators. Modification of orientational degrees of freedom of molecules was carried out in previous studies on water clusters[29–31] and nitrogen clusters.[32]

Geometry Optimization. The structures and energies of the CO_2 dimer and trimer in the MOM model given in ref 17 are consistent with the results reported by Weida et al.[33] Therefore, these clusters are not taken into account in this work. The global minima of the tetramer and pentamer were easily found by a random search method where many geometries randomly generated were optimized by the L-BFGS[25] method. On the other hand, the random search method located the same global minimum of $(CO_2)_6$ with a low probability (4 out of 1000 local optimizations). Therefore, to search optimal geometries of clusters for $n \ge 6$ efficiently, the optimization cycle shown in Figure 1 was repeated.[34] Table 1 lists the number of cycles performed for each cluster, that of the cycles where the same lowest-energy configuration is obtained, and the lowest-energy value E_n^{min}. The average number of local optimizations in a cycle was smaller than 50 for the clusters with the size of $6 \le n \le 40$.[35]

For the CO_2 clusters of 10, 20, 30, and 40 molecules, 100 cycles took approximately 3.2, 20.1, 56.5, and 119.1 min, respectively, on a 3 GHz Pentium IV processor. Geometry optimizations were executed in serial mode on a single processor and five processors were available for calculation.

TABLE 1: Number of Cycles (N) Performed in Geometry Optimization of $(CO_2)_n$ and the Number of Cycles (N_s) That Identify the Same Lowest-Energy Configuration with the Energy E_n^{min} (in kJ mol^{-1})

n	N	N_s	E_n^{min}	n	N	N_s	E_n^{min}	n	N	N_s	E_n^{min}
4[a]	100	27	−27.387	17	200	68	−241.312	29	40000	2	−461.613
5[a]	100	12	−40.734	18	200	49	−259.077	30	30000	2	−479.016
6	100	66	−55.790	19	200	49	−276.982	31	20000	2	−498.144
7	100	94	−70.475	20	1000	48	−294.373	32	35000	2	−516.908
8	100	73	−84.871	21	1000	27	−313.496	33	30000	2	−536.092
9	100	47	−101.158	22	1000	17	−331.935	34	312000	2	−556.802
10	200	52	−116.969	23	1000	11	−349.175	35	30000	2	−575.772
11	200	85	−133.780	24	1000	6	−366.325	36	40000	2	−594.746
12	200	137	−151.282	25	1000	9	−385.063	37	34000	3	−616.224
13	200	159	−173.447	26	4000	14	−404.105	38	26000	3	−635.237
14	200	155	−188.315	27	20000	9	−423.117	39	48000	2	−654.829
15	200	139	−206.411	28	20000	16	−444.842	40	25000	3	−677.635
16	200	102	−224.087								

[a] Random search was performed.

TABLE 2: Comparison of the Present Data with the Lowest-Energy Values Obtained in the Literature (in kJ mol^{-1})

n	this work	Liu and Jordan[18]	Maillet et al.[19,20]	Torchet et al.[21]	n	this work	Maillet et al.[19,20]	Torchet et al.[21]
6	−55.790	−55.81			25	−385.063		−380[a]
8	−84.871	−84.89			28	−444.842	−444.780	
13	−173.447	−173.47	−173.430		30	−479.016	−479[a]	
19	−276.982	−277.02	−275.931	−272[a]	32	−516.908	−517[a]	−509[a]
23	−349.175		−348.694		35	−575.772	−573[a]	

[a] Values estimated from the results shown in the literature.

TABLE 3: Number of Local Structures Found in CO_2 Clusters and Lennard-Jones Clusters

	$(CO_2)_n$						LJ_n		
n	(20/0)	(18/1)	(16/2)	(14/3)	(12/4)	(10/5)	(20/0)	(10/5)	(8/6)
13−18	1						1		
19	1						2		
20	2						2		
21, 22	1						2		
23, 24	1						3		
25				3			3		
26		1					4		
27	2	1					4		
28	1						4		
29, 30	1						5		
31	1		1				1	3	
32, 33	1	1					1	4	
34	1						1	4	
35			1	1	2		1	4	
36			1	1	1		1	5	
37				1	3	2	1	5	
38				1	2	3			6
39				1	2	3	1	6	
40				1	1	4	1	6	

Discussion

The E_n^{min} values for $n = 6$, 8, 13, 19, 23, and 28 are reported in refs 18–20. However, the lowest-energy values of the following clusters are not numerically presented: $(CO_2)_{30}$, $(CO_2)_{32}$, and $(CO_2)_{35}$ in ref 20, and the $(CO_2)_n$, $n = 19$, 25, and 32, clusters in ref 21. Their energies were estimated from the figures shown in the literature.[20,21] These data[18–21] are compared with the energies derived by the present method in Table 2.

The results reported by Liu and Jordan[18] are equal to those obtained in the present study within 0.04 kJ mol^{-1}. The slight energy differences between the minima obtained in the present study and in ref 18 are due to the values of the potential parameters because the geometries in the present study agree with those in ref 18. The energies of the 19-, 23-, and 35-molecule clusters calculated in the present study are lower than the values reported by Maillet et al.[19,20] by 1.1, 0.5, and 3 kJ mol^{-1}, respectively. The energies of $(CO_2)_n$, $n = 19$, 25, and 32, reported by Torchet et al.[21] are higher than the values in the present study by more than 5 kJ mol^{-1}. The capability of the present method to search lowest-energy configurations is superior to that of MD simulations adopted in refs 19–21.

The global minima of the other clusters under investigation are first proposed. To examine structural variation of the global minima, the local structure analysis[20] was carried out. The orientations of molecules were neglected and relative positions of carbon atoms (the centers of mass of CO_2 molecules) were analyzed as follows: (1) A carbon atom surrounded by 12 carbon atoms is searched. (2) If distances between a central atom and surrounding atoms are smaller than a cutoff distance, 5.2 Å,[20] the analysis proceeds to next step. Otherwise, return to step 1. (3) The surrounding carbon atoms construct a 12-vertex polyhedron. If an edge of the polyhedron is longer than 5.2 Å, it is neglected in next step. (4) The numbers of triangular and square faces, T and S, are counted and the notation (T/S) is used to characterize the polyhedron. The above steps are repeatedly performed for all the carbon atoms in a cluster. The characterization of CO_2 clusters for $n \geq 13$ is presented in Table 3.

The CO_2 clusters for $13 \leq n \leq 34$ are characterized by (20/0) and (18/1) local structures except for $(CO_2)_{25}$ and $(CO_2)_{31}$: the (20/0) and (18/1) local structures correspond to an icosahedron and a defective icosahedron, respectively. For larger clusters, (12/4) and (10/5) local structures are observed. The configurations of these clusters are shown in Figure 2 together with the crystal structure.[21,36] The relative arrangement of molecules in these clusters is similar to that in the crystal although the disorder in the configurations of the 35- and 36-molecule clusters is remarkably observed. Because six local structures identified in $(CO_2)_{40}$ lie in the surface, the (8/6) local structure (cuboctahedron) found in the crystal is not detected in the cluster. The lowest-energy configurations of the $(CO_2)_n$,

$n \leq 34$, clusters generally take icosahedral-like structures and those of the remaining clusters exhibit cuboctahedral-like character.

It is interesting to clarify the effect of the linear shape of the CO_2 molecule on the cluster geometries. In the present study, therefore, the results of the local structural analysis performed for LJ clusters[37] are compared with those for $(CO_2)_n$ in Table 3. The number of the (20/0) structures increases stepwise with increasing cluster size for LJ clusters for $n \leq 30$ and similar trend is found for the (10/5) structures in LJ clusters with the size of $31 \leq n \leq 40$. Therefore, the size dependence of geometries of $(CO_2)_n$ is considerably different from that of LJ_n.

The local structures including one or two pentagonal faces are also obtained in the global-minimum geometries of $(CO_2)_n$ with the size of $21 \leq n \leq 36$ whereas no pentagonal face is observed for LJ clusters. The above differences are considered to originate from the shape of particles in the clusters.

Recently, Jose and Gadre[38] reported the geometries of $(CO_2)_n$ with $n = 2-8$ by ab initio calculations. According to their investigation, the geometries for $n = 4-8$ are trigonal pyramidal, tetragonal pyramidal, tetragonal bipyramidal, pentagonal bipyramidal, and pentagonal bipyramidal with one molecule, respectively. The cluster geometries obtained in the present study are shown in Figure 3 and are consistent with the geometrical features mentioned above except for $n = 5$. In the MOM model, the geometry of the global minimum of the pentamer is trigonal bipyramidal. It is more stable than the tetragonal pyramidal configuration by 2.7 kJ mol^{-1} in energy.

As shown in Figure 3, the global minimum of $(CO_2)_{20}$ is a double icosahedron (two (20/0) local structures overlap each other) with one additional molecule. In the double icosahedron, a lot of pentagonal bipyramidal structures are included. Jose and Gadre[38] carried out a test calculation on the 20-molecule cluster and reported that its geometry showed pentagonal

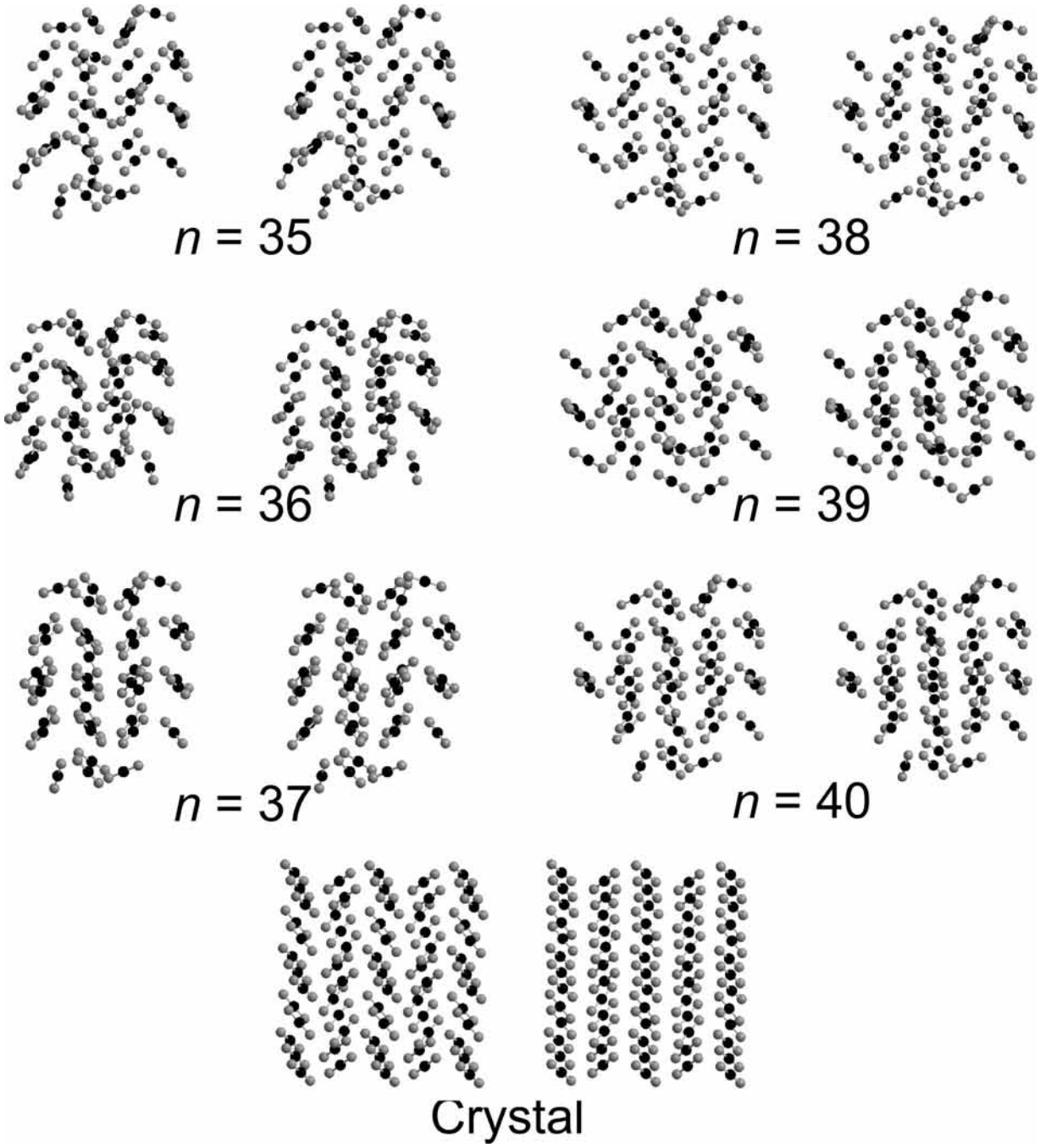

Figure 2. Stereographic views of the CO_2 crystal structure and the CO_2 clusters for $n = 35-40$ obtained in the present study.

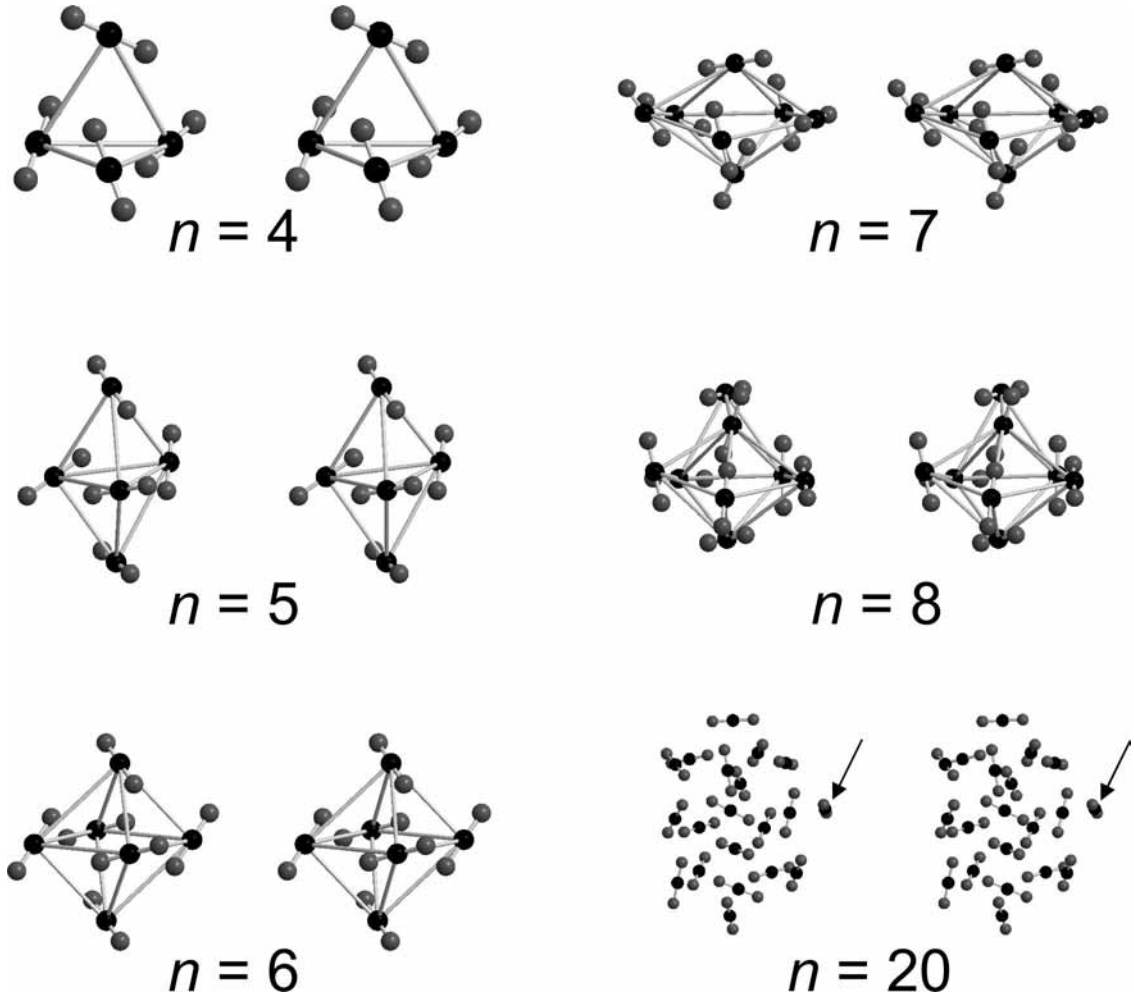

Figure 3. Stereographic views of the CO_2 clusters for $n = 4-8$, 20 obtained in the present study. Connectors between carbon atoms are drawn to understand shapes of the clusters for $n = 4-8$ easily. In the cluster for $n = 20$, a double icosahedron is constructed from the 19 carbon atoms except for the molecule indicated by the arrow.

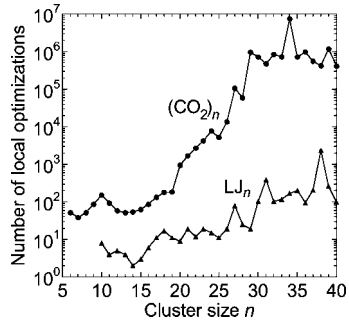

Figure 4. Number of local optimizations required for obtaining the global minimum of each cluster versus the cluster size n: circles, carbon dioxide cluster; triangles, Lennard-Jones cluster.

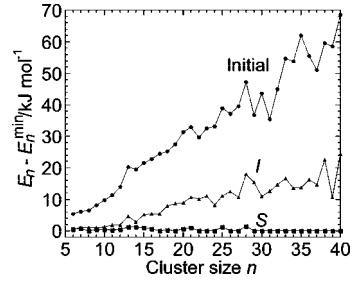

Figure 5. Differences of energies of initial optimized geometries (circles) and those of geometries optimized by using the I (triangles) and S (squares) operators from the global-minimum energies E_n^{min}.

bipyramidal patterns. Therefore, the geometry obtained in the present study qualitatively agrees with that in ref 38.

Figure 4 shows the number of local optimizations required for finding the global minimum of each cluster. It is approximately $10-10^5$ times larger than the number of local optimizations for the corresponding LJ cluster.[1] This indicates that the orientational degrees of freedom of CO_2 molecules significantly influence the number of local minima on potential energy surface. It is difficult to search the global minimum of $(CO_2)_{34}$ because the number of local optimizations needed for this cluster 7.5×10^6 is 1 order of magnitude larger than the numbers for the neighboring clusters.

To examine the efficiency of the I and S operators, the energies finally obtained by using these operators were averaged over all the cycles where global minima were searched. The results are shown in Figure 5 together with the energies obtained after the local optimizations of initial geometries.

The differences between the initial energies and the global-minimum energies E_n^{min} are approximately proportional to the cluster sizes. The energy differences $E_n - E_n^{min}$ are significantly reduced by the I operator and are furthermore decreased by the S operator. Therefore, the geometry modification due to these operators is excellent for lowering potential energies of CO_2 clusters. The $E_n - E_n^{min}$ values obtained by using the S operator are less than 1.5 kJ mol^{-1} and particularly zero for the clusters

with $n = 19$, 22−24, 26, 27, and 29−40. The global minima of the remaining clusters are obtained by using the *O* operator with probabilities of 0.015−0.82.

To examine if the number of repetitions of the *O* operator is insufficient for the clusters with $n = 19$, 22−24, 26, 27, and 29−40, the number of trials of the *O* operator was changed from 10 to 200, that is, $N_{fail} \leq 200$ for the *O* operator (see Figure 1 for the meaning of N_{fail}). Geometry optimization of $(CO_2)_{19}$ was carried out and the results showed no improvement on the performance of the present optimization method. Therefore, it must be difficult to search the global minima of the above clusters by using the *O* operator. The *O* operator is considered not to be useful for geometry optimization of larger clusters.

The study on geometry optimization of benzene clusters[10] shows that the *O* operator is efficient for most of the clusters for $n \leq 30$. Therefore, the efficiency of the *O* operator depends on constituents of clusters.

Conclusion

The heuristic and unbiased method based on the surface, interior, and orientational operators was used for geometry optimization of CO_2 clusters. Some global minima reported in the literature[18–20] were confirmed by the present method. In addition, the method improved global minima for $(CO_2)_{23}$, $(CO_2)_{25}$, and $(CO_2)_{35}$ and yielded new global minima for many CO_2 clusters.

Examination of the performance of the method shows that the ability of the *O* operator to search more stable configurations is rather limited. On the other hand, the *I* and *S* operators can efficiently search configurations with lower potential energies as indicated in the study[10] on benzene clusters. Therefore, the present method is still efficient for geometry optimization of small molecular clusters. An investigation on geometry optimization of water clusters is in progress.

Cluster configurations were analyzed by taking into account local structures of 12-vertex polyhedra. The analysis shows that the size dependence of the lowest-energy structures of $(CO_2)_n$ is different from that of LJ clusters. This is attributable to the shape of particles in the clusters.

Acknowledgment. This work was supported by the Grant-in-Aid for Scientific Research (C) (No. 19550001) from Japan Society for the Promotion of Science (JSPS).

Supporting Information Available: Cartesian coordinates and stereographic views of the global minima obtained in the present study. This information is available free of charge via the Internet at http://pubs.acs.org.

References and Notes

(1) Takeuchi, H. *J. Chem. Inf. Model.* **2006**, *46*, 2066.
(2) Romero, D.; Barrón, C.; Gómez, S. *Comput. Phys. Commun.* **1999**, *123*, 87.
(3) Shao, X.; Jiang, H.; Cai, W. *J. Chem. Inf. Comput. Sci.* **2004**, *44*, 193.
(4) Xiang, Y.; Jiang, H.; Cai, W.; Shao, X. *J. Phys. Chem. A* **2004**, *108*, 3586.
(5) Xiang, Y.; Cheng, L.; Cai, W.; Shao, X. *J. Phys. Chem. A* **2004**, *108*, 9516.
(6) Barrón, C.; Gómez, S.; Romero, D.; Saavedra, A. *Appl. Math. Lett.* **1999**, *12*, 85.
(7) Wales, D. J.; Doye, J. P. K. *J. Phys. Chem. A* **1997**, *101*, 5111.
(8) Shao, X.; Xiang, Y.; Cai, W. *J. Phys. Chem. A* **2005**, *109*, 5193.
(9) Wales, D. J.; Doye, J. P. K.; Dullweber, A.; Hodges, M. P.; Naumkin, F. Y.; Calvo, F.; Hernández-Rojas, J.; Middleton, T. F. The Cambridge Cluster Database, http://www-wales.ch.cam.ac.uk/CCD.html (accessed January 2008).
(10) Takeuchi, H. *J. Chem. Inf. Model.* **2007**, *47*, 104.
(11) Pullan, W. J. *J. Chem. Inf. Comput. Sci.* **1997**, *37*, 1189.
(12) White, R. P.; Niesse, J. A.; Mayne, H. R. *J. Chem. Phys.* **1998**, *108*, 2208.
(13) Easter, D. C. *J. Phys. Chem. A* **2003**, *107*, 2148.
(14) Easter, D. C. *J. Phys. Chem. A* **2003**, *107*, 7733.
(15) Williams, D. E. *Acta Crystallogr., Sect. A* **1980**, *36*, 715.
(16) van de Waal, B. W. *Chem. Phys. Lett.* **1986**, *123*, 69.
(17) Bukowski, R.; Sadlej, J.; Jeziorski, B.; Jankowski, P.; Szalewicz, K.; Kucharski, S. A.; Williams, H. L.; Rice, B. M. *J. Chem. Phys.* **1999**, *110*, 3785.
(18) Liu, H.; Jordan, K. D. *J. Phys. Chem. A* **2003**, *107*, 5703.
(19) Maillet, J.-B.; Boutin, A.; Buttefey, S.; Calvo, F.; Fuchs, A. H. *J. Chem. Phys.* **1998**, *109*, 329.
(20) Maillet, J.-B.; Boutin, A.; Fuchs, A. H. *J. Chem. Phys.* **1999**, *111*, 2095.
(21) Torchet, G.; de Feraudy, M.-F.; Boutin, A.; Fuchs, A. H. *J. Chem. Phys.* **1996**, *105*, 3671.
(22) Murthy, C. S.; O'Shea, S. F.; McDonald, I. R. *Mol. Phys.* **1983**, *50*, 531.
(23) van de Waal, B. W. *J. Chem. Phys.* **1987**, *86*, 5660.
(24) The r_e value was calculated from the Lennard-Jones potential parameters taken from the following literature: Cuadros, F.; Cachadiña, I.; Ahumada, W. *Mol. Eng.* **1996**, *6*, 319.
(25) Liu, D. C.; Nocedal, J. *Math. Prog.* **1989**, *45*, 503.
(26) Shao, X.; Yang, X.; Cai, W. *J. Comput. Chem.* **2008**, *29*, 1779.
(27) The number of repetition is safely set to be $3n$ because the number of distinct spaces is empirically found to be $\approx 1.5n$.
(28) The cases with $m \geq 2$ must be carefully treated. If the distances between the selected positions are close to r_e, slight changes of the positions and orientations may introduce a large energy variation.
(29) Wales, D. J.; Hodges, M. P. *Chem. Phys. Lett.* **1998**, *286*, 65.
(30) Niesse, J. A.; Mayne, H. R. *J. Comput. Chem.* **1997**, *18*, 1233.
(31) Bandow, B.; Hartke, B. *J. Phys. Chem. A* **2006**, *110*, 5809.
(32) Calvo, E.; Torchet, G.; de Feraudy, M.-F. *J. Chem. Phys.* **1999**, *111*, 4650.
(33) Weida, M. J.; Sperhac, J. M.; Nesbitt, D. J. *J. Chem. Phys.* **1995**, *103*, 7685.
(34) The maximum numbers of *m* were 5 and 4 for the *I* and *S* operators, respectively, referring to the study on LJ and benzene clusters. For small clusters with $8 \geq n \geq 6$, however, the maximum number of the moved molecules was reduced to be $n-4$.
(35) Partial geometry optimizations were used in steps 2 and 5 in the *S* operator. They were not counted in the number of local optimizations because partial optimization was much faster than full geometry optimization.
(36) Keesom, W. H.; Köhler, J. W. L. *Physica (Utrecht)* **1934**, *1*, 655.
(37) The potential energy of LJ_n is expressed in this work as $E_{LJ} = \sum_{i=1}^{n-1} \sum_{j=i+1}^{n} (1/r_{ij}^{12} - 2/r_{ij}^{6})$. The cutoff distance used in the local structure analysis is taken to be 1.1, a value slightly larger than equilibrium distance.
(38) Jose, K. V. J.; Gadre, S. R. *J. Chem. Phys.* **2008**, *128*, 124310.

JP802872P